

2008

## Dynamics of Directed Boolean Networks under Generalized Elementary Cellular Automata Rules, with Power-Law Distributions and Popularity Assignment of Parent Nodes

Ray Goodman  
*University of Nebraska at Omaha*

Mihaela T. Velcsov  
*University of Nebraska at Omaha, dvelcsov@unomaha.edu*

Follow this and additional works at: <https://digitalcommons.unomaha.edu/mathfacpub>

 Part of the [Mathematics Commons](#)

Please take our feedback survey at: [https://unomaha.az1.qualtrics.com/jfe/form/SV\\_8cchtFmpDyGfBLE](https://unomaha.az1.qualtrics.com/jfe/form/SV_8cchtFmpDyGfBLE)

---

### Recommended Citation

Goodman, Ray and Velcsov, Mihaela T., "Dynamics of Directed Boolean Networks under Generalized Elementary Cellular Automata Rules, with Power-Law Distributions and Popularity Assignment of Parent Nodes" (2008). *Mathematics Faculty Publications*. 81.  
<https://digitalcommons.unomaha.edu/mathfacpub/81>

This Article is brought to you for free and open access by the Department of Mathematics at DigitalCommons@UNO. It has been accepted for inclusion in Mathematics Faculty Publications by an authorized administrator of DigitalCommons@UNO. For more information, please contact [unodigitalcommons@unomaha.edu](mailto:unodigitalcommons@unomaha.edu).

# Dynamics of Directed Boolean Networks under Generalized Elementary Cellular Automata Rules, with Power-Law Distributions and Popularity Assignment of Parent Nodes

**Ray Goodman**

*Department of Computer Science,  
University of Nebraska at Omaha, Omaha, NE 68198-2184*

**Mihaela T. Matache\***

*Department of Mathematics,  
University of Nebraska at Omaha, Omaha, NE 68182-0243*

---

This study provides an analysis of the dynamics of fixed-size directed Boolean networks governed by generalizations of elementary cellular automata rules 22 and 126, under a power-law distribution of parent nodes and a popularity parent assignment. The analysis shows the existence of a two-piece chaotic attractor for smaller values of the power-law parameter which evolves into a “cloud”-like attractor for larger values of the parameter. Values of the parameter for which the system exhibits an ordered behavior are indicated as well. The dynamics are investigated using space-time diagrams, delay plots, bifurcation diagrams, and Lyapunov exponent computations. It is also shown that the children (out)links do not obey a power-law distribution; more precisely, numerical investigations indicate that the children links have a Gaussian-like distribution.

---

## 1. Introduction

A significant amount of work has been performed during the past few years related to nondirected Boolean networks in which the connectivity of the nodes is governed by a power-law distribution. Such networks led to the so-called scale-free networks in which highly connected vertices have a larger chance to occur than in the small-world network model introduced by Watts and Strogatz [1] and variations of it generated by authors such as Serra *et al.* [2], or in the classical random graph model introduced by Erdős and Rényi [3]. The probability of finding a highly connected vertex decreases exponentially with the connectivity in these two models, whereas in scale-free networks the probability decreases according to a power-law. The important work of Barabási *et al.* in [4]

---

\*Electronic mail address: [dmatache@mail.unomaha.edu](mailto:dmatache@mail.unomaha.edu).

was a turning point in the modeling and analysis of certain real networks. The existence of scale-free networks, or in general small-world networks, has been identified in many real situations such as biological networks in Jeong *et al.* [5], social networks in Wasserman and Faust [6], or computer networks and the World Wide Web in Albert *et al.* [7], and Barabási *et al.* [8]. For example, Aldana and Cluzel show that a certain class of scale-free networks is more robust to perturbations than a classical Kauffman network in which every element interacts, on average, with say  $K$  other elements of the network [9]. In that paper, although the network is directed (i.e., the number of inputs is not necessarily equal to the number of outputs for each node), the power-law distribution can be used for either the distribution of input connections or that of the output connections (or both). The authors focus on a Boolean rule that assigns randomly a value of 0 or 1 to each node, with fixed probability, regardless of the number of inputs or their actual values. By contrast, in this paper we assume that the nodes evolve according to rules that represent generalizations of certain elementary cellular automata (ECA) rules. In particular we will focus on ECA rules 22, 126, and a special rule called the rule of density of ones that is described later. At the same time, the network considered in this paper evolves according to a power-law distribution for the input connections paired with a preferential choice of the parent nodes based on the nodes' popularity. We are interested in identifying the distribution of the output connections and the dynamical behavior of a system governed by the number of parents generated using a power-law paired with a popularity parent selection, and evolving according to the ECA rules indicated. Thus we consider a case of a directed network which is more common in real life than bidirectional networks. Moreover, directed networks have been far less studied in the literature compared to undirected networks. However, they have been shown to occur in complex networks such as cells, networks of chemicals linked by chemical reactions, or the Internet as observed by Albert and Barabási [10], metabolic networks as seen by Jeong *et al.* [5], or transcriptional networks as observed by Yook *et al.* [11].

Scale-free networks emerge in the context of a growing network in which new vertices connect preferentially to the more highly connected vertices in the network as shown by Barabási and Albert [12], and Amaral *et al.* [13]. Examples of networks obtained by a preferential attachment of links include the World Wide Web as shown in Barabási *et al.* [8], the complex node attachments in biological and artificial neural networks in Shiner and Davison [14], and Watt's small-world network [1], derived from Milgram's small-world problem [15, 16]. Typically the number of connections of a new vertex is a fixed constant. It has been shown by Amaral *et al.* [13] that the introduction of certain constraints, such as inactive vertices obtained either by aging or by reaching a maximum number of links, may lead to cutoffs in the

power-law decay of the tail of the connectivity distribution or even a suppression of a power-law region [13]. In this paper, we include an upper bound for the size of the network, and therefore the number of links of a given node is bounded. This leads to a distribution of the outgoing (children) links that is not a power-law, but has a bell shape.

Research has also shown that chaos can occur in random Boolean networks. For example, Matache *et al.* [17–21] explore the behavior of networks governed by generalized ECA rule 126 through mean field models of the probability of finding a node in state 1 or ON at time  $t$ . This is done for synchronous or asynchronous networks, with a fixed or variable number of parents that are assigned randomly. In this paper we explore the behavior of networks evolving under the constraints specified earlier by considering the actual network, as opposed to an associated mathematical model, despite the fact that this approach can be cumbersome due to the more involved computations. A network with  $N$  nodes has a set of  $2^N$  possible states.

The networks presented in this paper fall in the category of the so-called quenched networks since the Boolean functions do not change with time; also the inputs to the Boolean functions are fixed but randomly chosen among the existing nodes (except for the ECA parent assignment). On the other hand the category of annealed networks implies that at each time step the Boolean functions and their inputs are randomly chosen. Studies such as the well-known book by Kauffman [22], or the paper by Derrida and Pomeau [23], have shown that the quenched and annealed models exhibit very similar dynamics of state transitions, especially for large networks. Thus one could deal with any of the two approaches (under suitable hypotheses) and obtain results that are valid for the other approach as well.

The goals of this paper are to first describe the children distribution of a directed network of size  $N$  in which the number of parents is given by a power-law distribution and the parents are assigned based on node popularity and then analyze the dynamics of such a network evolving under certain generalized ECA rules.

In section 2 we describe the network in detail and introduce the power-law distribution, the parent assignment procedure, and the Boolean rules used. Then in section 3 we consider the probability distribution of the children (out)links. In section 4 we study the dynamics of the network under various scenarios using space-time diagrams, delay plots, Lyapunov exponent computations, and bifurcation diagrams. We finish with conclusions and further directions of investigation.

## 2. Network description

---

In this section we describe the network. Namely, we discuss the power-law distribution of parent nodes and their assignment. Then we focus

on the actual Boolean rules used to determine the evolution of nodes from one time step to the next.

### ■ 2.1 The power-law parent distribution

We consider a network with  $N$  nodes so that each node can be in one of two states 0 or 1 at any time  $t$ . The evolution of node  $i$  from time  $t$  to  $t + 1$  is determined by the states of the nodes in the target node's neighborhood, that is, by its parent nodes. The number of parents is generated using a truncated power-law distribution,

$$P(k) = \frac{1}{\zeta(\gamma)k^\gamma} \quad k = 1, 2, \dots, N \quad (1)$$

where  $\zeta(\gamma) = \sum_{k=1}^N 1/k^\gamma$  is the scaling factor. The parameter of the distribution is  $\gamma > 0$ . Thus each node is assigned  $k$  parents with probability  $P(k)$ .

The parameter  $\gamma$  is varied in steps of 0.01, from 1 to 3 and thus various networks are constructed and their behavior analyzed. This covers the ranges of  $\gamma$  typically found in complex networks. For example, in the case of scale-free networks the usual range is  $2 < \gamma \leq 3$ , while  $1 < \gamma < 2$  is typical for biological networks (e.g., genes, proteins, and metabolism).

### ■ 2.2 Parent assignment

We assume that each node is its own parent. So if a node  $i$  has a total of  $k+1$  parents, then only the remaining  $k$  parents need to be assigned. The parent assignment is achieved through a popularity procedure. Popularity is based on the number of children nodes associated with each node, that is, the number of nodes for which the node under consideration is a parent. More precisely, the popularity of a node is the proportion of the number of its children to the total number of children in the system. We will call this quantity the node popularity probability (NPP).

The NPP is defined for each node  $i$  as follows:

$$\text{NPP}_i = \frac{C_i}{\sum_{n=1}^N C_n} \quad (2)$$

where  $C_n$  is the number of children of node  $n$ ,  $n = 1, 2, \dots, N$ .

The parents are assigned in order from node 1 to node  $N$ , so the NPP of each node may change at each step of the parent selection.

In the simulations we compare this parent assignment procedure with a random parent assignment in which the  $k$  parents of a node are randomly selected from the  $N$  nodes of the network with probability  $1/\binom{N}{k}$ , as well as an ECA assignment with exactly three parents: node  $i$  itself together with nodes  $i - 1$  and  $i + 1$ .

### ■ 2.3 Boolean rules

Once all the parents of all nodes are assigned, we are interested in evolving the network according to various Boolean rules.

Three different rules are tested: generalized cellular automaton rule 22, generalized cellular automaton rule 126, and a rule based on the density of ones. In the simulations, each of the rules is processed on the initial node data sets using varying initial conditions for 200 time steps. We assume a synchronous update of all nodes. Future work will focus also on asynchronous networks.

As observed in [17] rule 126 is one of several which exhibit randomly distributed triangular shapes of arbitrarily large size. This makes rule 126 a class III complexity generating rule [24]. Rule 126 is both legal, reflection symmetric and quiescent, and totalistic, where the rule depends only on the relative number of ON and OFF states and not their order [25]. There are 32 legal rules and 16 totalistic rules. Only eight of these rules, including rule 126, are in both classes: 0, 22, 104, 126, 128, 150, 232, and 254. They separate into Wolfram's four classes as class I: 0, 128, 254; class II: 104, 232; class III: 22, 126, 150; and class IV: none. Besides the automata in classes I and II which have relatively simple behavior [24], this leaves only three: 22, 126, and 150. But rule 150 is additive (linear in algebraic form) which simplifies its analysis by transferring unusual effects from the structure of the automata to the initial conditions only. As well as rules 22 and 126 both being in Wolfram's class III, they are also both in the same  $\kappa = 2$  in a new classification, regarding separating planes for the basic eight-point hypercube (along with rule 104) [26].

Both rules 126 and 22 have a natural and simple interpretation in terms of the growth of cell colonies. For rule 126, complete crowding of live, ON, cells causes death, OFF, in the next generation. Complete isolation of a potential cell prevents birth in the next generation. A similar interpretation holds for rule 22, it just is not quite as complete.

It is natural then to study these rules and extend them to networks of an arbitrary size  $N$ . We do this as follows.

#### **Generalized cellular automaton rule 22**

The generalized cellular automaton rule 22 is based on Wolfram's ECA rule 22 [24]. Wolfram's rule is defined for a node that has three parents. If one and only one of the parent nodes has a state of 1, then the child node will have its state set to 1. We use the following generalization applicable to any number of parent nodes: if the proportion of nodes in state 1 in the target node's neighborhood is nonzero and less than  $1/3$ , then the node will be set to 1 at the next time point, otherwise, it will be set to 0. Hung *et al.* [27] have used a straightforward generalization of rule 22, namely a node is turned ON if and only if a single node is ON in the neighborhood of the node under consideration. They use this rule

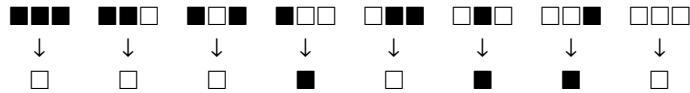


Figure 1. ECA rule 22.

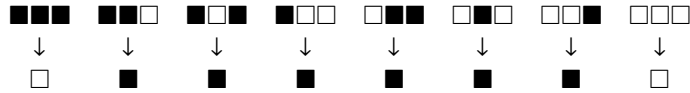


Figure 2. ECA rule 126.

in the context of synchronizing stochastically coupled random Boolean networks. The extension used in this paper is more general. Figure 1 shows the ECA rule 22.

#### Generalized cellular automaton rule 126

The generalized cellular automaton rule 126 is based on Wolfram's ECA rule 126. If the state of all of the parent nodes is either 0 or 1; that is, the nodes are all ON or all OFF, then the child node will have its state set to 0 or OFF (i.e., complete crowding or complete isolation generates death in the next time step). Observe that this rule can be easily applied to any number of parent nodes without any further changes, and has been studied in [17–21] for a network in which the number of parents is either fixed or variable and in which the parents are chosen randomly. However, no previous paper involves a power-law parent distribution paired with a popularity based parent assignment. Figure 2 represents the ECA rule 126.

#### Density of ones rule

The third Boolean rule we use is called density of ones and is a further generalization of rules 22 and 126. The rule states that a certain percentage of the parent nodes must be in state 1, for the child node to be set to 1 at the next time point. The density of ones for node  $i$  at time  $t$  is defined as:

$$d_i(t) = \frac{1}{k_i} \sum_{n=1}^{k_i} c_n(t) \quad (3)$$

where  $i$  identifies the node under consideration,  $c_n(t)$  is the state of the parent node  $n$  at time  $t$ , and  $k_i$  is the number of parents of node  $i$ .

The rule is stated as

$$c_i(t+1) = \begin{cases} 1 & \text{if } 0 < d_i(t) < P \\ 0 & \text{otherwise} \end{cases} \quad (4)$$

where  $P \in (0, 1]$  is a fixed parameter.

Observe that  $P = 1$  is the generalized ECA rule 126, while  $P = 1/3$  yields the generalized ECA rule 22.

### 3. The distribution of children links

Given the procedure described in section 2, we generate a variety of networks for various values of  $\gamma$ . In Figure 3 we generate a log–log plot of the parent and child distributions for two separate values of the power-law parameter, namely  $\gamma = 1.6$  and  $\gamma = 2.6$ . The network has  $N = 256$  nodes and for practical purposes the number of parents is at least three. Observe the almost linear plot of the parent distribution which corresponds to a power-law distribution in a log–log plot. However, the children distribution is far from linear, which suggests that it is not a power-law. Thus, when the links are directed, and the power-law distribution of parents is paired with a popularity assignment of parents, the resulting children distribution clearly departs from a power-law.

We provide fit plots for the children distribution in the case  $\gamma = 1.6$ , using the actual frequencies instead of the log–log plots. Figure 4 shows the results of using the distribution fit feature of Matlab® [28]. It can be

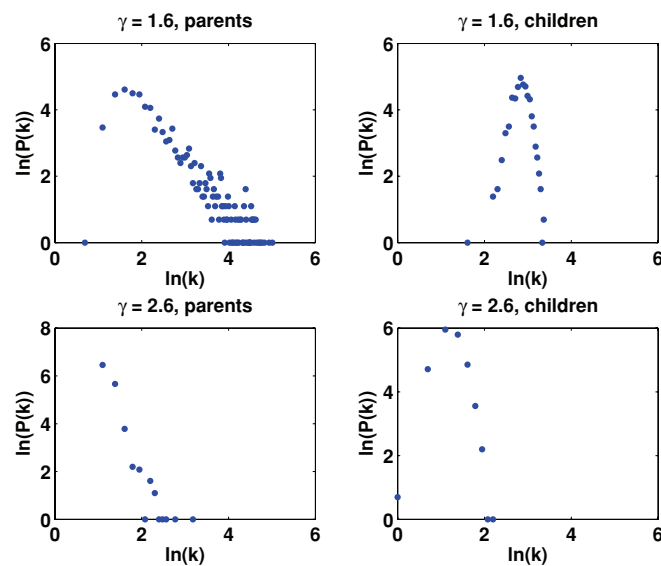


**Figure 3.** Parent and children empirical distributions obtained from a network with  $N = 256$  nodes, in which the number of parents is generated with a power-law distribution with parameter  $\gamma = 1.6$  and  $\gamma = 2.6$  as specified in the plots. The parents are assigned based on popularity. The results in these graphs are obtained by averaging over a number of realizations of the network with a given  $\gamma$ . We observe a clear departure of the children distribution from a power-law.

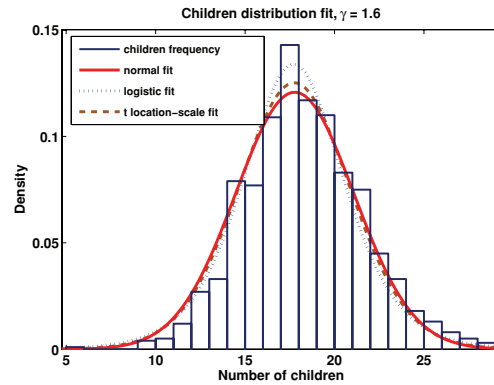


**Figure 4.** Children empirical probability distribution obtained from a network with  $N = 256$  nodes, in which the number of parents is generated with a power-law distribution with parameter  $\gamma = 1.6$ . The fit is obtained using a normal, a logistic, and a  $t$  location-scale distribution. The parameters of the fitted distributions are estimated as follows: normal with  $\mu = 17.8$  and  $\sigma = 3.3$ ; logistic with  $\mu = 17.7$  and  $\sigma = 1.87$ ;  $t$  location-scale with  $\mu = 17.7$ ,  $\sigma = 3.15$ , and  $\nu = 22.4$ . Observe the similarities between the fitted distributions.

observed that several different distributions provide a reasonably good fit: a  $t$  location-scale distribution (which is known to be applicable for heavy tailed distributions), a normal, and a logistic distribution. All of them are plotted on the same graph for easy comparison.

Recall that the  $t$  location-scale probability density is given by

$$f(x) = \frac{\Gamma(\frac{\nu+1}{2})}{\sigma\sqrt{\nu\pi}\Gamma(\frac{\nu}{2})} \left[ \frac{\nu + \left(\frac{x-\mu}{\sigma}\right)^2}{\nu} \right]^{-((\nu+1)/2)}$$

with location parameter  $\mu$ , scale parameter  $\sigma > 0$ , and shape parameter  $\nu > 0$ . This distribution approaches the normal distribution as  $\nu \rightarrow \infty$ , and smaller values of  $\nu$  yield heavier tails. Recall also that if  $X$  is a  $t$  location-scale random variable, then  $(X - \mu)/\sigma$  has a Student's  $t$  distribution with  $\nu$  degrees of freedom.

We recall the logistic distribution as well. A random variable  $X$  has a logistic distribution if its probability density function is of the type

$$f(x) = \frac{e^{(x-\mu)/\sigma}}{\sigma(1 + e^{(x-\mu)/\sigma})^2}$$

with location parameter  $\mu$  and scale parameter  $\sigma > 0$  for all real  $x$ . This distribution has longer tails and a higher kurtosis than the normal distribution.

The parameters of the fitted distribution are indicated in the caption of Figure 4 and are obtained using a maximum likelihood estimation

procedure. Given that both the logistic and the  $t$  location-scale distributions approach a normal distribution for certain parameter behavior, we can deduce that the children distribution is close in shape to a Gaussian distribution.

To understand if the empirical observations are supported by the actual mathematical distribution of children, we observe that the number of children links evolves in time according to the following formulae.

- At time  $t = 0$ , we have that  $C_i(t) = 1, \forall i = 1, 2, \dots, N$ . This is because in the beginning the  $N$  nodes are set as parents (children) of themselves.
- At time  $t > 0$ , the  $k_t$  parents of node  $C_t$  obtained from a power-law distribution with parameter  $\gamma$  are assigned according to the popularity procedure. This means that the number of children of node  $t$  does not change, so  $C_t(t) = C_t(t - 1)$ , while the number of children of any other node changes as follows:

$$C_i(t) = C_i(t - 1) + k_t \cdot \text{NPP}_i(t), \quad \text{where} \quad \text{NPP}_i(t) = \frac{C_i(t - 1)}{\sum_{j \neq t} C_j(t - 1)}. \quad (5)$$

It is easy to see that

$$\sum_{i=1}^N C_i(t) = N + k_1 + k_2 + \dots + k_t \quad (6)$$

as expected since once  $k_t$  parents are selected,  $k_t$  new children links are formed as well. Thus the total number of children links in the network at time  $t$  is given by equation (6).

Observe that the given formulae can be written as a composition  $g = g^N \circ g^{N-1} \circ \dots \circ g^2 \circ g^1$  of maps

$$g^t : \mathbf{R}^N \rightarrow \mathbf{R}^N$$

given by

$$g^t(p_1, p_2, \dots, p_N) = (g_1^t(p_1, p_2, \dots, p_N), g_2^t(p_1, p_2, \dots, p_N), \dots, g_N^t(p_1, p_2, \dots, p_N))$$

where

$$g_t^t(p_1, p_2, \dots, p_N) = p_t$$

and

$$g_i^t(p_1, p_2, \dots, p_N) = p_i + k_t \frac{p_i}{N + k_1 + k_2 + \dots + k_t - p_i} \quad \text{for } i \neq t.$$

Since the network starts with the initial condition  $(p_1, p_2, \dots, p_N) = (1, 1, \dots, 1)$  we are interested in  $g(1, 1, \dots, 1)$ . More precisely, we would like to determine the distribution of the  $i$ th component of this composition.

Notice that the computations become cumbersome from the very first step of the composition. However, the results are in terms of sums of the type  $k_1 + k_2 + \dots + k_N$  which represent values of independent and identically distributed random variables with the same power-law parameter. It is known [29] that this kind of sum converges to a Lévy distribution as  $N$  increases, by the central limit theorem. Recall also that Lévy distributions (and in particular Gaussian distributions which are a special case of Lévy distributions) are stable since they are “fixed points” of the convolution operation, and are also attractors. Any distribution convoluted with itself a large number of times converges to a stable law. In general, Lévy distributions have heavier tails than Gaussian distributions, although they have the same symmetric shape. They are useful in describing multiscale phenomena; that is, when both very large and very small values of a quantity can commonly be observed, as stated in [29]. Although we cannot conclude that the final distribution is Lévy or Gaussian given that the computations also involve other transformations of the independent and identically distributed random variables giving the number of parents at each time  $t$ , we can expect a Lévy- or Gaussian-like distribution given the empirical results obtained so far. Observe that repeated compositions yield transformations of the type: sums, differences, products, quotients, or squares of independent power-law distributions, which clearly may lead to distributions that are not of the power-law type. To understand the combined effect of these transformations, we perform a numerical investigation of the final distribution as follows.

We perform the composition numerically for the given initial condition with various values of the parameter  $\gamma$ . Thus we start with a network with  $N = 256$  nodes for simplicity and compute  $g^{256} \circ g^{255} \circ \dots \circ g^2 \circ g^1(1, 1, \dots, 1)$  for 10,000 different sets of parents  $\{k_1, k_2, \dots, k_{256}\}$  with a given  $\gamma$ . Then we generate a density plot of these 10,000 repetitions for each of the 256 nodes on the same graph. In Figure 5 we provide these plots for  $\gamma = 1, 1.2, 1.4, 1.6, 1.8, 2, 2.2, 2.4, 2.6, 2.8$ , and 3 respectively. The graphs become more narrow and are condensed to the left with increased  $\gamma$ . Since all 256 density plots for each given value of  $\gamma$  are very similar and overlap a lot, we can see that any node has a generic bell-shaped children distribution.

To emphasize the Gaussian-like distribution, we select node 1 and plot its distribution in the form of a histogram with a fitted normal distribution on top in Figure 6. We do this for  $\gamma = 1, 1.2, 1.4, 1.6$ , and 1.8 only for more clarity. Observe that indeed the normal distribution provides a very good fit. Thus we conclude that a power-law parent distribution paired with a popularity parent assignment for directed networks of finite size generates a Gaussian-like distribution for the number of children.

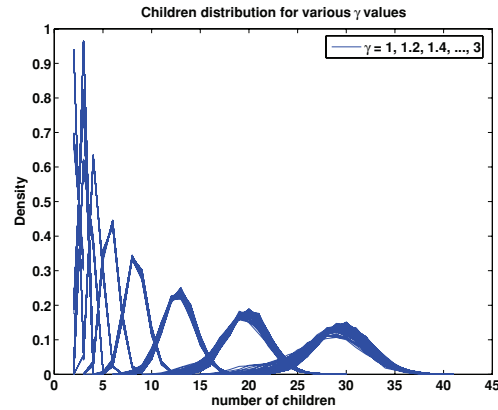


**Figure 5.** Children probability distribution obtained from a network with  $N = 256$  nodes, in which the number of parents is generated with a power-law distribution with parameter  $\gamma = 1, 1.2, 1.4, \dots, 3$ . The distribution for each of the 256 nodes is graphed and we observe the similarities of the distributions for distinct values of  $\gamma$ . We conclude that there is a unique children distribution that corresponds to any node of the network given that the plots are very similar or overlap for all of the 256 nodes and any given  $\gamma$ . We also observe that as  $\gamma$  increases the graphs tend to become more narrow and to condense to the left of the graph. We also note the bell-shaped graphs.

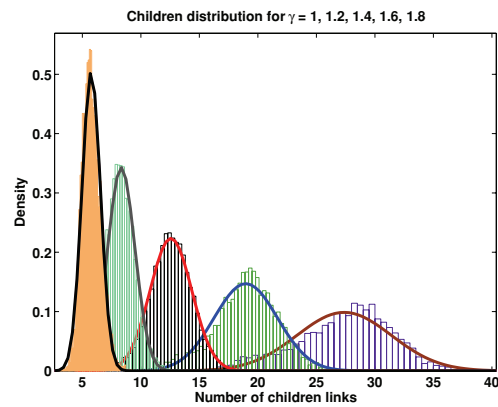


**Figure 6.** Children probability distribution obtained from a network with  $N = 256$  nodes, in which the number of parents is generated with a power-law distribution with parameter  $\gamma = 1, 1.2, 1.4, 1.6, \text{ and } 1.8$ . The distribution for node 1 is graphed and a fitted normal distribution is plotted on top. We observe the excellent match which supports the conclusion that the children distribution is bell shaped.

In section 4 we are interested in the dynamics generated by networks obtained as described and evolved under the generalized ECA rules mentioned earlier.

#### 4. Network dynamics

In this section we describe and provide samples of the extensive simulations performed on networks generated according to the rules presented. We study the dynamics of the network through an analysis of the frequency of active nodes (i.e., nodes in state 1) paired with delay plots, Lyapunov exponents, and bifurcation diagrams.

For the purposes of this study, various initial node sets are created based on the power-law distribution and the popularity model discussed earlier. Each network consists of  $N = 256$  nodes with the number of parent nodes assigned based on different  $\gamma$  values using the power-law distribution. The values for  $\gamma$  range from 1.00 to 3.00 and are tested in steps of 0.01. The number of parents assigned to each node is in the range of 3 to 256. Once the number of parents is determined for each node of the network, the parent nodes are then assigned based on the popularity model.

In addition to the varying parent node configurations, the initial state of the network is also under consideration. Each node could initially be in state 1 or 0. In order to test various initial conditions of the network, the concentration of nodes in state 1 is varied from  $1/N$  (i.e., only one node is initially in state 1) to 1 (i.e., all nodes are initially in state 1). Except for this last case, the nodes to be set to 1 are randomly selected from the  $N$  nodes. Thus if the frequency of ones is  $J/N$  then  $J$  nodes are selected from the  $N$  nodes of the network with probability  $1/\binom{N}{J}$ .

The algorithms for node initialization, dataset generation, rule implementations, time step processing, and analysis were developed utilizing Matlab [28]. Procedures for saving the data sets to Microsoft Excel<sup>®</sup> were also created.

We compare the popularity method of assigning parent nodes to random parent assignment and ECA parent assignment with exactly three parents. In the figures that follow we show three choices for the power-law parameter  $\gamma$ , namely 1.2, 1.6, and 2.6, that yield typical graphs.

First, let us take a look at some pattern formation plots obtained by evolving a network with  $N = 100$  nodes in a space-time diagram. Based on numerous simulations, we note that larger networks yield similar results and the quality of the rule evolution does not change with the size of the network (provided that the network is large enough), the number of time steps, the random parent assignment for say a fixed  $\gamma$ , or the initial conditions. Thus, as long as the parents are assigned randomly and the network is large enough, the subnetwork topologies

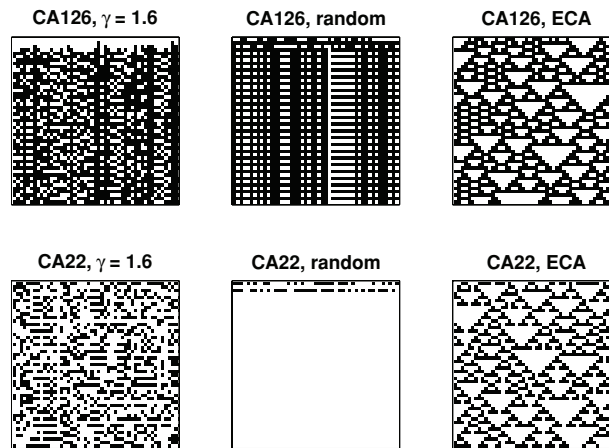


**Figure 7.** Pattern formation plots (space-time diagrams) for a network of  $N = 100$  nodes evolved according to the specified generalized ECA rules and the specified parent assignment (popularity, random, and ECA). Observe the differences between the plots. The generalized ECA rule 22 generates zeros for a random parent assignment which is a typical feature as observed by the authors in numerous experiments.

yield similar overall dynamical behavior for a given rule and parameter selection. However, a change of parameter can yield a modification of the behavior. At the same time we note that if the network is small, the correlations between nodes become more significant, and the patterns may indicate an orderly behavior with convergence to a fixed state or a cycle of states. In Figure 7 we present a network evolving under the generalized ECA rule 126 in the first line and the generalized ECA rule 22 in the second line. The first column is obtained under the popularity method for parent assignment with the number of parents given by a power-law with  $\gamma = 1.6$ , the second column is obtained using a random parent assignment, while the third column represents the usual ECA neighborhood of three parents. We observe the differences in the evolution of the network under the six different scenarios, and the rather ordered evolution under the random parent assignment with convergence to zero for the generalized ECA rule 22. This is a feature observed for most cases of random parent assignment as we will indicate later. As  $\gamma$  increases more order is observed in the plots. We will supplement these plots with the analysis that follows.

Next we provide 200 time steps of the network evolution for five different rules. The rules are: density of ones 50%, density of ones 20%, density of ones 80%, generalized ECA rule 126 (CA 126), and generalized ECA rule 22 (CA 22). At each time step the density (or frequency) of ones, labeled  $x(t)$ , is calculated and plotted as a percentage in the

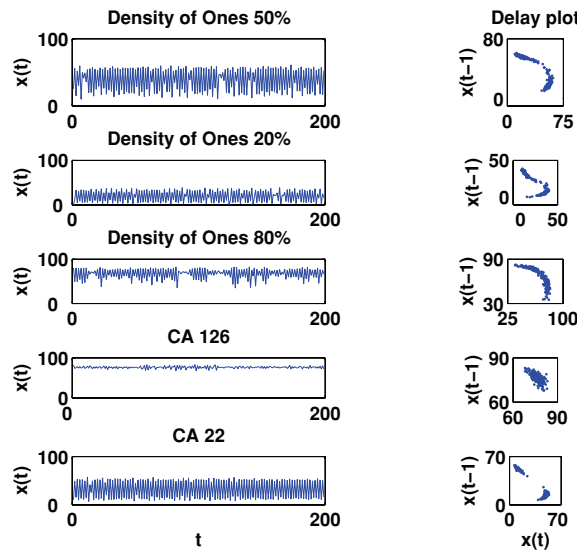


**Figure 8.** Frequency of nodes in state 1 and corresponding time-1 delay plots for a network with 256 nodes, evolved 200 time steps, with a power-law parent distribution with  $\gamma = 1.2$ . Each line represents a different rule as specified in the titles of the first column.

first column of Figures 8 through 11. The second column in each figure represents the corresponding time-1 delay plot of the number of ones, that is, the plot of  $x(t-1)$  versus  $x(t)$ . The delay plots are a useful graphical tool that can reproduce the periodic orbit of the system space and can indicate the existence of stable or chaotic attractors. For example, if stability is reached and  $x(t) = x(t-1)$  for all  $t$ , then the plot would show only one point. Similarly, two points indicate a stable period two orbit. On the other hand, a collection of points that do not follow a clear pattern could suggest the existence of chaos, or chaotic attractors.

Observe that increasing  $\gamma$  makes it less likely to have a large number of parents. It can be seen that for smaller  $\gamma$  values most of the plots are spread out, while for  $\gamma = 2.6$  the plots are tighter for some of the scenarios considered. Observe the rather clear chaotic attractors for  $\gamma = 1.2$ . For the ECA parent assignment we observe order only for density of ones 20%, in which case the frequency of ones converges to zero. For the random parent assignment the frequency of ones converges to zero in all cases, except CA 126 for which the plot is similar to that of CA 22 for  $\gamma = 1.2$ , but with higher values of the frequency. We do not include a separate figure for this case. Note also that larger values of  $\gamma$  mean that most of the nodes will have exactly three parents as in the case of ECA. However, the parents need not be the immediate

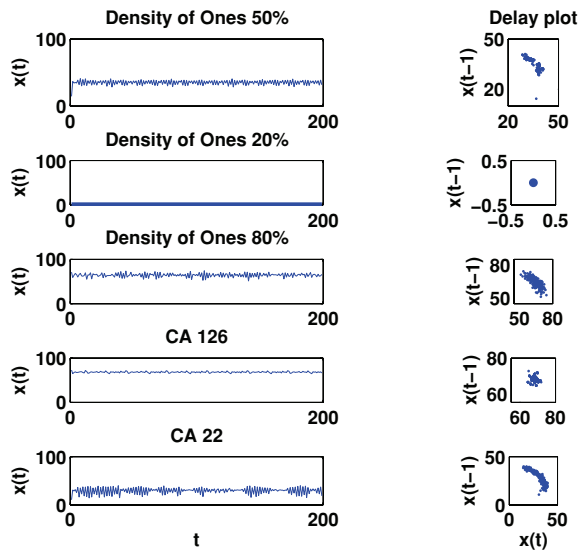


**Figure 9.** Frequency of nodes in state 1 and corresponding time-1 delay plots for a network with 256 nodes, evolved 200 time steps, with a power-law parent distribution with  $\gamma = 1.6$ . Each line represents a different rule as specified in the titles of the first column.

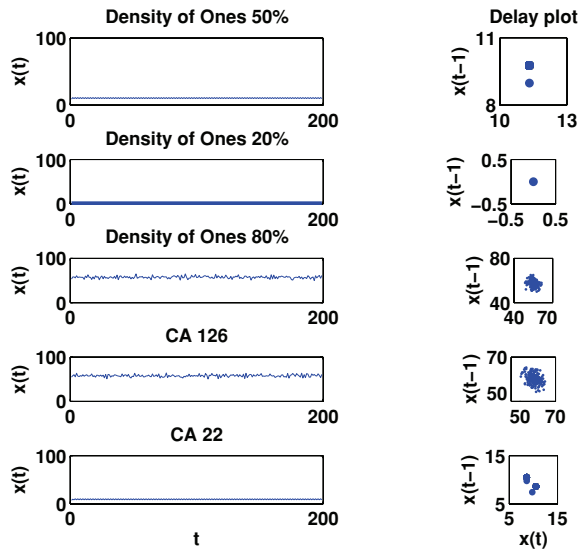


**Figure 10.** Frequency of nodes in state 1 and corresponding time-1 delay plots for a network with 256 nodes, evolved 200 time steps, with a power-law parent distribution with  $\gamma = 2.6$ . Each line represents a different rule as specified in the titles of the first column.

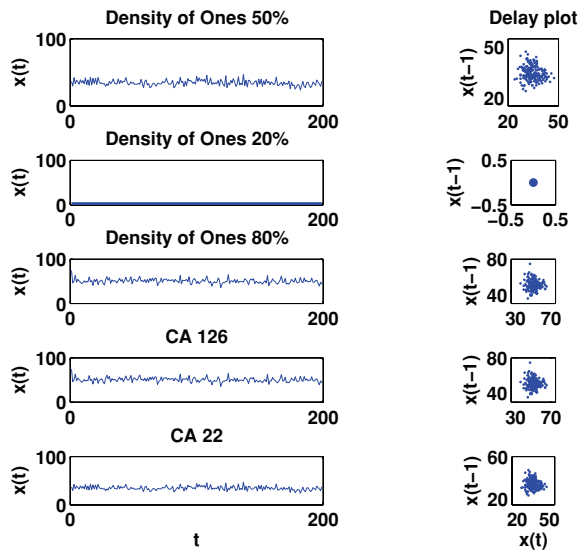


**Figure 11.** Frequency of nodes in state 1 and corresponding time-1 delay plots for a network with 256 nodes, evolved 200 time steps, such that each node  $i$  has three parents, namely nodes  $i - 1$ ,  $i$ ,  $i + 1$ , which represents the case of the classical ECA. Each line represents a different rule as specified in the titles of the first column.

neighbors of the nodes or the nodes themselves, so the case of large  $\gamma$  resembles a spatially scrambled ECA. We observe that the delay plots corresponding to these two situations are in general tighter and some exhibit fixed points, as in Figures 10 and 11.

We now focus on Lyapunov exponent computations for a one-dimensional time series as in our case. A time series is said to be chaotic if the series is not asymptotically periodic and the Lyapunov exponent (LyE) is greater than zero [30]. The LyE is a measure of the rate of separation of two points that are in the same neighborhood. A positive LyE indicates the points of the time series are diverging, while a negative LyE indicates the points are coming closer together. The LyE can be generated by taking two nearby orbits and calculating the logarithmic rate of separation of the orbits. We briefly explain how this is done following the terminology of [31, 32].

For example, consider two orbits, a “reference” orbit and a “test” orbit, separated at time  $t_0$  by a small phase space distance  $D(t_0)$ . If we denote by  $D(t)$  the distance between the points of these two orbits at time  $t$ , then the LyE can be expressed as

$$\lambda = \lim_{t \rightarrow \infty} \frac{1}{t - t_0} \ln \frac{D(t)}{D(t_0)}.$$

CA 22	CA 126	Density of Ones 20%	Density of Ones 50%	Density of Ones 80%
Popularity $\gamma = 1.2$				
$0.260 \pm 0.111$ <i>Not Periodic</i>	$0.454 \pm 0.099$ <i>Not Periodic</i>	$0.436 \pm 0.131$ <i>Not Periodic</i>	$0.411 \pm 0.120$ <i>Not Periodic</i>	$0.540 \pm 0.133$ <i>Not Periodic</i>
Popularity $\gamma = 1.6$				
$0.409 \pm 0.106$ <i>Not Periodic</i>	$0.175 \pm 0.180$ <i>Not Periodic</i>	No LyE Converges	$0.066 \pm 0.079$ <i>Not Periodic</i>	$0.610 \pm 0.090$ <i>Not Periodic</i>
Popularity $\gamma = 2.6$				
$-0.028 \pm 0.112$ Periodic	$0.713 \pm 0.095$ <i>Not Periodic</i>	No LyE Converges	$-0.051 \pm 0.102$ Periodic	$0.593 \pm 0.100$ <i>Not Periodic</i>
Neighborhood 3 parents				
$0.437 \pm 0.094$ <i>Not Periodic</i>	$0.503 \pm 0.119$ <i>Not Periodic</i>	No LyE Converges	$0.437 \pm 0.094$ <i>Not Periodic</i>	$0.503 \pm 0.119$ <i>Not Periodic</i>
Random 3 parents				
No LyE Converges	$0.004 \pm 0.007$ Periodic	No LyE Converges	No LyE Converges	No LyE Converges

**Table 1.** Lyapunov exponents and periodicity. LyE are calculated utilizing the software Chaos Data Analyzer. The LyE values are expressed as a value with an estimated error. Italics indicate chaos since the time series is nonperiodic and exhibits positive LyE. Observe that chaos is present mostly for smaller values of  $\gamma$ , whereas for the random parent assignment the behavior is mostly ordered. In some cases the software could not produce a LyE, while in other cases the error obtained for the LyE is larger and thus one has to take care when drawing conclusions.

In practice, we cannot afford infinitely long time spans, so we instead calculate the instantaneous LyE

$$\lambda(t) = \frac{1}{t - t_0} \ln \frac{D(t)}{D(t_0)}$$

after waiting long enough for  $\lambda(t)$  to settle to approximately its asymptotic value. For an actual computation of the instantaneous LyE from a time series see [31] or [32]. The algorithm explained in those papers is implemented in the Chaos Data Analyzer software [33] which is used in this study for calculations of the LyE as shown next.

Table 1 shows the resulting LyE with a calculated error (shown as LyE  $\pm$  error). The table also shows which data sets converge to a single point (labeled “Converges”), to a periodic orbit (labeled “Periodic”), or are nonperiodic (labeled “Not Periodic”), based on simulations. The combination of a positive LyE and nonperiodic orbits indicate chaotic behavior in the system. Observe that this occurs mostly for smaller values of  $\gamma$ .

To continue this analysis, a bifurcation diagram is created for rules CA 22, CA 126, and density of ones 50% against the parameter  $\gamma$ . Networks of 256 nodes are generated and the number of parents de-

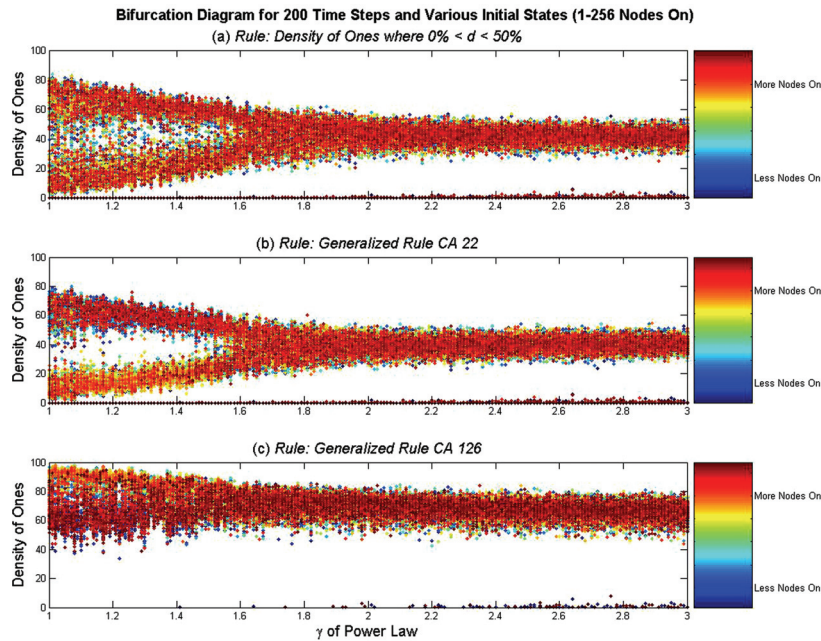


**Figure 12.** Bifurcation diagram for rules CA 22, CA 126, and density of ones 50% against the parameter  $\gamma$ .

terminated by using the power-law distribution and assigned utilizing the popularity model. In total, 201 different networks are generated, one for each of the  $\gamma$  values from 1.00 to 3.00. Each network is initialized and iterated 200 time steps. The resulting density of ones for the 200th iteration is graphed against  $\gamma$ , producing the bifurcation diagram in Figure 12. The shades of colors displayed indicate the number of nodes that are initially in state 1, as specified at the right of each graph. From the diagrams, we can identify a reversed bifurcation as  $\gamma$  approaches 1.6. This supports the observations of mostly chaotic behavior.

To further investigate this behavior and the chaotic attractors, delay plots are created again for each of the rules used for the bifurcation diagram for a unified view. The initial density of ones used for each of the delay plots in Figure 13 is 50/256 which shows the delay plots for each of the rules by lines. The rule is indicated in the left plot of each line. For simplicity, plots are generated only for  $\gamma = 1, 1.5, 2,$  and  $2.5$ . The plots show the strange attractors that are split for  $\gamma < 1.60$ . Around  $\gamma = 1.60$ , the split in the attractor vanishes. This supports the observations in the bifurcation diagram and previous delay plots.

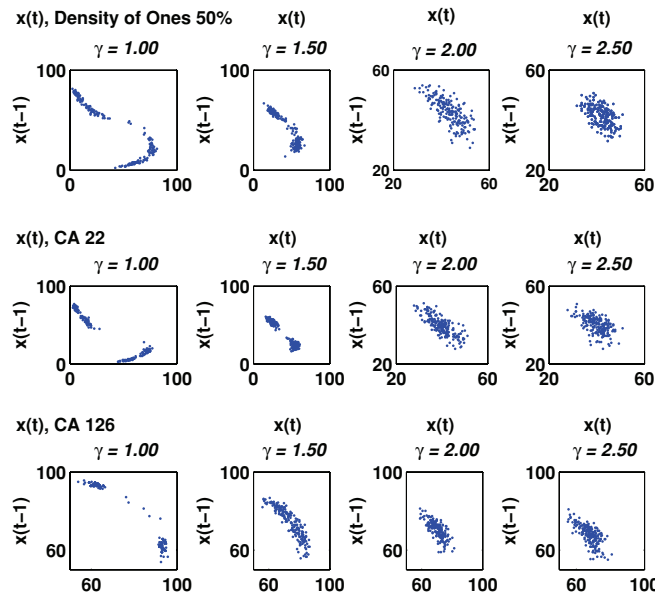


**Figure 13.** Time-1 delay plots for each of the three rules used in the bifurcation diagram of Figure 12. Four representative values of  $\gamma$  are displayed for each rule, namely  $\gamma = 1, 1.5, 2, 2.5$ , and the rules are specified above each row of plots. For all the rules we observe an evolution from a two-piece attractor to a cloud-like attractor as  $\gamma$  increases. These plots support the results displayed in the bifurcation diagram.

### 5. Conclusions

This study provides an analysis of the dynamics of directed Boolean networks governed by various extensions of elementary cellular automata (ECA) rules, under a power-law distribution of parents and a popularity parent assignment in comparison to a random or ECA parent assignment. The analysis shows that chaos can occur in more instances under the scenario of the popularity parent assignment with a smaller power-law parameter than in the other cases considered. The existence of a two piece chaotic attractor is observed for smaller values of the power-law parameter which evolves into a “cloud”-like attractor for larger values of the parameter. It is shown that the distribution of the children links is Gaussian-like. These results have significance, for example, in the development of artificial neural networks and in understanding the behavior in more complex biological neural networks.

Further study is required that can model more complex behaviors, such as varying rules on different nodes, asynchronous processing of time steps, and performing additional analysis of synchronization properties of such networks.

At the same time it would be useful to identify a suitable mathematical model for say the density map associated to a Boolean network evolving according to the generalized rule 22 or the density of ones rule. This work has actually started and one of the authors has provided an analysis of a mathematical density map for a further generalization of these two rules in [34] and identified the dynamics of the network under various parameter combinations. In that model, corresponding to a quenched network, it is assumed that the parent nodes act independently, so the correlations between the Boolean functions and their inputs are ignored as in the case of annealed networks. A noise procedure is also applied to study robustness to perturbations. The quenched and the annealed dynamics are equivalent in that scenario.

It would also be of interest to analyze the robustness to asynchronism or noise induction of such networks. Similar studies have been performed such as Fatès and Morvan [35] where robustness to asynchronism of one-dimensional ECA is studied using a statistical approach, Cornforth *et al.* [36] where various updating schemes are shown to affect the overall dynamics and that global synchronization can arise from local temporal coupling, and Goodrich and Matache [21] who study the robustness to noise induction of a synchronous Boolean network governed by ECA rule 126. In [34] a stochastic noise procedure is applied to analyze the robustness of Boolean networks under certain forms of the generalized rule 22 and to identify possible dynamical phase transitions. Further studies could extend this analysis to more sophisticated generalizations.

At the same time the topic of synchronization of chaotic networks, in particular scale-free networks, has applications in physics, complex systems, electrical engineering and laser physics, neuroscience and biology as observed by Newth and Brede in [37] where they study the fitness landscape of coupled oscillators over several types of networks including scale-free. They provide an optimization algorithm to determine network structures that lead to an enhanced ability to synchronize. Although their approach involves differential equations, it would be interesting to use some of their ideas and techniques in studying the synchronization properties of networks considered in this paper.

An additional area of interest is modeling the concept of node–parent degradation and reassignment. This is a phenomenon that is observed in biological neural networks when synapses between neurons, strengthen (long-term potentiation) and weaken (long-term depression), including the establishment of new node connections and dissolution of lesser used connections. This phenomenon is being utilized in today’s artificial neural networks to simulate the learning process. It would take this research closer to understanding the extent to which an annealed approximation is similar to the quenched network in this paper.

**References**

- [1] D. J. Watts and S. H. Strogatz, "Collective Dynamics of 'Small-World' Networks," *Nature*, **393** (1998) 440–442.
- [2] R. Serra, M. Villani, and L. Agostini, "A Small-World Network Where All Nodes Have the Same Connectivity, with Application to the Dynamics of Boolean Interacting Automata," *Complex Systems*, **15**(2) (2004) 137–155.
- [3] P. Erdős and A. Rényi, "On the Evolution of Random Graphs," *Publications of the Mathematical Institute of the Hungarian Academy of Sciences*, **5** (1960) 17–61.
- [4] A. L. Barabási, R. Albert, and H. Jeong, "Mean-Field Theory for Scale-Free Random Networks," *Physica A*, **272** (1999) 172–187.
- [5] H. Jeong, B. Tombor, R. Albert, Z. N. Oltvai, and A. L. Barabási, "The Large-Scale Organization of Metabolic Networks," *Nature*, **407** (2000) 651–654.
- [6] S. Wasserman and K. Faust, *Social Network Analysis* (Cambridge University Press, Cambridge, UK, 1994).
- [7] R. Albert, H. Jeong, and A. L. Barabási, "Diameter of the World-Wide Web," *Nature*, **401** (1999) 130–131.
- [8] A. L. Barabási, R. Albert, and H. Jeong, "Scale-Free Characteristics of Random Networks: The Topology of the World-Wide Web," *Physica A*, **281** (2000) 69–77.
- [9] M. Aldana and P. Cluzel, "A Natural Class of Robust Networks," *Proceedings of the National Academy of Sciences*, **100**(15) (2003) 8710–8714.
- [10] R. Albert and A. L. Barabási, "Statistical Mechanics of Complex Networks," *Review of Modern Physics*, **74** (2002) 47–97.
- [11] S.-H. Yook, Z. N. Oltvai, and A. L. Barabási, "Functional and Topological Characterization of Protein Interaction Networks," *Proteomics*, **4**(4) (2004) 928–942.
- [12] A. L. Barabási and R. Albert, "Emergence of Scaling in Random Networks," *Science*, **286** (1999) 509–512.
- [13] L. A. N. Amaral, A. Scala, M. Barthélémy, and H. E. Stanley, "Classes of Small-World Networks," *Proceedings of the National Academy of Sciences*, **97**(21) (2000) 11149–11152.
- [14] J. S. Shiner and M. Davison, "Quantifying the Connectivity of Scale-Free and Biological Networks," *Chaos, Solitons, and Fractals*, **21** (2004) 1–8.
- [15] S. Milgram, "The Small World Problem," *Psychology Today*, May 1967, 60–67.

- [16] J. Travers and S. Milgram, "An Experimental Study of the Small World Problem," *Sociometry*, **32** (1969) 425.
  - [17] M. T. Matache and J. Heidel, "Random Boolean Network Model Exhibiting Deterministic Chaos," *Physical Review E*, **69**, 056214 (2004) 10 pages.
  - [18] M. T. Matache and J. Heidel, "Asynchronous Random Boolean Network Model Based on Elementary Cellular Automata Rule 126," *Physical Review E*, **71**, 026232 (2005) 13 pages.
  - [19] X. Deng, H. Geng, and M. T. Matache, "Dynamics of Asynchronous Random Boolean Networks with Asynchrony Generated by Stochastic Processes," *BioSystems*, **88** (2007) 16–34.
  - [20] M. T. Matache, "Asynchronous Random Boolean Network Model with Variable Number of Parents Based on Elementary Cellular Automata Rule 126," *International Journal of Modern Physics B*, **20** (2006) 897–923.
  - [21] C. S. Goodrich and M. T. Matache, "The Stabilizing Effect of Noise on the Dynamics of a Boolean Network," *Physica A*, **379** (2007) 334–356.
  - [22] S. A. Kauffman, *The Origins of Order: Self-Organization and Selection in Evolution* (Oxford University Press, New York, 1993).
  - [23] B. Derrida and Y. Pomeau, "Random Networks of Automata: A Simple Annealed Approximation," *Europhysics Letters*, **1** (1986) 45–49.
  - [24] S. Wolfram, *A New Kind of Science* (Wolfram Media Inc., Champaign, IL, 2002).
  - [25] S. Wolfram, "Statistical Mechanics of Cellular Automata," *Review of Modern Physics*, **55** (1983) 601.
  - [26] L. O. Chua, S. Yoon, and R. Dogaru, "A Nonlinear Dynamics Perspective of Wolfram's New Kind of Science. Part I: Threshold of Complexity," *International Journal of Bifurcation and Chaos*, **12**(12) (2002) 2655–2766.
  - [27] Y-C. Hung, M-C. Ho, J-S. Lih, and I-M. Jiang, "Chaos Synchronization of Two Stochastically Coupled Random Boolean Networks," *Physics Letters A*, **356** (2006) 35–43.
  - [28] MATLAB software by The MathWorks, Natick, MA.
  - [29] J.-P. Bouchaud and M. Potters, *Theory of Financial Risks. From Statistical Physics to Risk Management* (Cambridge University Press, 2000).
  - [30] K. T. Alligood, T. D. Sauer, and J. A. Yorke, *CHAOS An Introduction to Dynamical Systems* (Springer-Verlag, New York, Heidelberg, Berlin, 1996).
  - [31] A. Wolf, J. B. Swift, H. L. Swinney, and J. A. Vastano, "Determining Lyapunov Exponents from a Time Series," *Physica D*, **16** (1985) 285–317.
- Complex Systems*, **14** (2008) 357–379

- [32] M. A. Murison, “Notes on How to Numerically Calculate the Maximum Lyapunov Exponent,” Astronomical Applications Department, U. S. Naval Observatory, Washington DC, 1995.  
<http://www.alpheratz.net/murison/papers/Notes/LyapCalc/LyapCalc.pdf>
- [33] Chaos Data Analyzer (CDA) software by Julien C. Sprott and George Rowlands, distributed by Physics Academic Software, Raleigh, NC.
- [34] G. L. Beck and M. T. Matache, “Dynamical Behavior and Influence of Stochastic Noise on Certain Generalized Boolean Networks,” submitted.
- [35] N. A. Fatès and M. Morvan, “An Experimental Study of Robustness to Asynchronism for Elementary Cellular Automata,” *Complex Systems*, **16**(1) (2005) 1–27.
- [36] D. Cornforth, D. G. Green, and D. Newth, “Ordered Asynchronous Processes in Multi-Agent Systems,” *Physica D*, **204** (2005) 70–82.
- [37] D. Newth and M. Brede, “Fitness Landscape Analysis and Optimization of Coupled Oscillators,” *Complex Systems*, **16**(4) (2006) 317–331.